Hexokinase-2 Expression in ^{11}C-Methionine–Positive, ^{18}F-FDG–Negative Multiple Myeloma

Stefan Kircher[1,2], Antje Stolzenburg[3], Klaus Martin Kortüm[4], Malte Kircher[3], Matteo Da Via[4], Samuel Samnick[3], Andreas K. Buck[3], Hermann Einsele[4], Andreas Rosenwald[1,2], and Constantin Lapa[3]

[1]Institute of Pathology, University of Würzburg. Würzburg, Germany; [2]Comprehensive Cancer Center Mainfranken, Würzburg, Germany; [3]Department of Nuclear Medicine, University Hospital Würzburg, Würzburg, Germany; and [4]Department of Hematology and Oncology, University Hospital Würzburg, Würzburg, Germany

PET with ^{18}F-FDG is the standard modality in nuclear medicine for imaging multiple myeloma (MM). However, viable MM as detected by MRI or PET with other metabolic tracers, including ^{11}C-methionine, may be missed—for example, because of low hexokinase 2 (HK2) expression of tumor cells. The aim of this study was to further investigate potential reasons for PET false negativity. **Methods:** A cohort of 15 mainly pretreated patients with relapsed or refractory biopsy-proven, serologically active MM who underwent both ^{18}F-FDG and ^{11}C-methionine PET/CT was retrospectively analyzed. **Results:** In 9 of the 15 patients, ^{18}F-FDG PET was negative in the presence of viable disease. In the remaining 6 patients, both ^{18}F-FDG and ^{11}C-methionine PET/CT revealed the same number of MM lesions. At immunohistochemistry, ^{18}F-FDG–negative myeloma did not exhibit significant differences in HK2 or glucose-6-phosphatase expression from ^{18}F-FDG–positive disease (P = 0.57 and P = 0.44, respectively). **Conclusion:** Beyond HK2 expression, ^{18}F-FDG negativity in (mainly pretreated) MM patients seems to be associated with additional causes not yet known.

Key Words: multiple myeloma; glucose-6-phosphatase; ^{11}C-methionine; ^{18}F-FDG; PET/CT

J Nucl Med 2019; 60:348–352
DOI: 10.2967/jnumed.118.217539

PET with ^{18}F-FDG as the standard nuclear medicine imaging modality is increasingly used in the diagnosis, prognostication, and management of multiple myeloma (MM) (*1–7*). Although sensitivity is generally high, particularly in extramedullary disease (*8*), subsets of viable malignant plasma cells might not be ^{18}F-FDG–avid and therefore might be missed by standard PET imaging (*4,9*). Recently, so-called false-negative ^{18}F-FDG PET results have been reported in 11% of patients with viable disease detectable on diffusion-weighted MRI and were linked to low hexokinase 2 (HK2) gene expression (*10*).

Potentially more sensitive approaches using radiolabeled tracers targeting metabolic pathways other than glycolysis or membrane receptors expressed by MM cells have been investigated, including ^{11}C-/^{18}F-choline (*11,12*) and ^{11}C-acetate (*13*) as markers of cell membrane lipid turnover and lipid metabolism.

In addition, we and others have reported on ^{18}F-FDG–negative, viable myeloma detectable with PET using ^{11}C-methionine, a radiolabeled amino acid (*14–19*). The aim of this study was to further investigate the underlying biology of metabolically active, so-called ^{18}F-FDG false-negative MM.

MATERIALS AND METHODS

We analyzed all patients with biopsy-proven, serologically active MM who underwent both ^{18}F-FDG and ^{11}C-methionine PET/CT as part of a previously published prospective study (*16*) approved by the local ethics committee (University of Würzburg). Of the entire cohort, patients with exclusively ^{11}C-methionine–positive (and ^{18}F-FDG–negative) disease were identified and compared with those who presented with identical results for both imaging examinations. All subjects gave written informed consent to sequential ^{18}F-FDG and ^{11}C-methionine PET/CT imaging in accordance with the Declaration of Helsinki. ^{11}C-methionine was administered under the conditions of the pharmaceutical law (German Medicinal Products Act, AMG §13 2b) according to German law and the responsible regulatory body (Regierung von Oberfranken).

In total, 9 patients (4 female; mean age, 59 ± 10 y) with exclusively ^{11}C-methionine–positive disease were identified and compared with 6 (control) subjects (1 female; mean age, 61 ± 8 y) in whom both PET tracers revealed an identical number of focal lesions, as well as tumor burden at identical sites. Thirteen of the 15 patients presented with relapsed or refractory, progressive disease, and the remaining two (patient 3 from the ^{18}F-FDG–negative cohort and patient C2 from the ^{18}F-FDG–positive cohort) presented with newly diagnosed, treatment-naïve disease. Imaging was performed before an intended change in therapy (in relapsed or refractory disease) or before treatment initiation (in the newly diagnosed cases). All patients had undergone recent (within 1 wk before PET imaging) random bone marrow biopsy of the iliac crest for histopathologic workup. The patients' characteristics are detailed in Table 1.

PET/CT was performed after injection of 302 ± 30 MBq of ^{18}F-FDG or 658 ± 143 MBq of ^{11}C-methionine, and the images were qualitatively and semiquantitatively analyzed as previously described (*16*).

The imaging results were compared with HK2 and glucose-6-phosphatase (G6Pase) expression of the myeloma cells as assessed by standard immunohistochemistry testing on trephine biopsies. The following antibodies were used: rabbit anti-HK2 (HPA028587 [Sigma-Aldrich]; dilution, 1:50 with Dako Advanced) and rabbit anti-G6Pase (ab83690 [Abcam]; dilution, 1:50 with Dako Advanced). For staining for HK2, healthy myocardium served as a positive control. For G6Pase, hepatocytes served as a reference. For both enzymes, vascular endothelium and mesenchymal stromal cells were used as

Received Jul. 11, 2018; revision accepted Oct. 10, 2018.
For correspondence or reprints contact: Constantin Lapa, University Hospital Würzburg, Department of Nuclear Medicine, Oberdürrbacher Strasse 6, D-97080 Würzburg, Germany.
E-mail: lapa_c@ukw.de
Published online Nov. 2, 2018.

TABLE 1
Patients' Characteristics

Patient no.	Age (y)	Sex	Myeloma type	Disease duration	IMID	PI	Auto SCT	BM involvement at time of PET (%)	Serum M protein (g/L)	Involved serum FLC level (mg/L)	^{18}F-FDG PET	No. of FL	^{11}C-methionine PET	No. of FL
^{18}F-FDG–negative														
1	67	M	IgG λ	14	Yes	Yes	Yes	15	29.2	20.4	Neg	—	Pos	20
2	56	M	IgA κ	32	Yes	Yes	Yes	40	44.7	0.5	Neg	—	Pos	>50
3	63	M	LC λ	0	No	No	No	15	0	444	Neg	—	Pos	>50
4	62	M	IgG κ	199	Yes	Yes	Yes	20	13.0	14,015	Neg	—	Pos	>50
5	53	F	LC κ	122	Yes	Yes	Yes	15	0	99	Neg	—	Pos	6
6	63	F	LC λ	23	No	Yes	Yes	10	0	1,876	Neg	—	Pos	>50
7	53	F	LC λ	11	Yes	Yes	No	20	0	3,396	Neg	—	Pos	>50
8	64	M	LC κ	54	Yes	Yes	Yes	25	0	1,183	Neg	—	Pos	16
9	62	F	IgG κ	39	Yes	No	Yes	10	1.7	955	Neg	—	Pos	5
^{18}F-FDG–positive														
C1	64	M	IgG κ	4	No	Yes	No	40	51.1	293	Pos	>50	Pos	>50
C2	63	M	LC κ	0	No	No	No	70	0	14,014	Pos	>50	Pos	>50
C3	51	M	IgG κ	34	Yes	Yes	Yes	60	24.6	828	Pos	>50	Pos	>50
C4	73	M	IgG κ	72	Yes	Yes	Yes	70	4.7	25,100	Pos	>50	Pos	>50
C5	63	F	IgG κ	22	Yes	Yes	Yes	30	47.5	1,907	Pos	>50	Pos	>50
C6	53	M	LC λ	57	Yes	Yes	Yes	0*	0	105	Pos	>50	Pos	>50

*Sampling error.

IMID = immunomodulatory drugs; PI = proteasome inhibitors; auto SCT = autologous stem cell transplantation; BM = bone marrow; FLC = free light chain; FL = focal lesions on PET/CT; neg = negative; pos = positive.

Disease duration is given in months (patients 3 and C2 presented with newly diagnosed disease). Bone marrow involvement was assessed by histologic evaluation of random iliac crest biopsy samples.

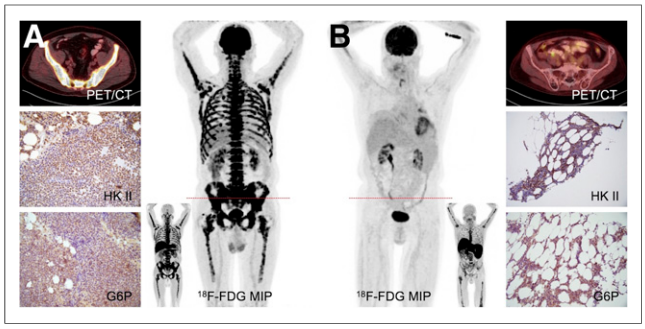

FIGURE 1. Example of ^{18}F-FDG–positive disease (A, patient C1) in comparison to ^{18}F-FDG–negative viable myeloma (B, patient 4). Shown are maximum-intensity projection (MIP) of ^{18}F-FDG and ^{11}C-methionine (inset) PET/CT, as well as immunohistochemistry results for HK2 and G6Pase from iliac crest biopsies (PET/CT). Both subjects presented with serologically progressive myeloma. Despite pronounced differences in imaging, both patients display almost equally high HK2 expression (IRS, 12 vs. 12) and G6Pase expression (IRS, 6 vs. 8).

negative controls. The stained sections were analyzed semiquantitatively by light microscopy according to the immunoreactive score (IRS) of Remmele and Stegner (*20*). The percentage of HK2- and G6Pase-positive cells was scored as follows: 0 (no positive cells), 1 (<10% positive cells), 2 (10%–50% positive cells), 3 (>50%–80% positive cells), 4 (>80% positive cells). Additionally, the intensity of staining was graded: 0 (no color reaction), 1 (mild reaction), 2 (moderate reaction), 3 (intense reaction). Multiplication of both scores for a given sample yielded the IRS classification: 0–1 (negative), 2–3 (mild), 4–8 (moderate), 9–12 (strongly positive). Statistical analysis was performed using the Student *t* test (GraphPad Prism, version 5.0).

An analysis of glucose transporter 1 and L-type amino acid transporter 1 (CD98) expression as the major routes of transport of ^{18}F-FDG and ^{11}C-methionine into the myeloma cell had already been performed (*17*).

RESULTS

Because of the selection criteria, ^{11}C-methionine PET/CT was positive in all 15 patients whereas ^{18}F-FDG did not reveal any active lesions in 9 of the 15 patients (Fig. 1). On a lesion basis, ^{11}C-methionine detected more than 50 focal lesions in 5 of these 9 ^{18}F-FDG PET–negative patients, 20 lesions in a single patient, and less than 20 focal lesions in the remaining 3 patients. Patient 3 presented with ^{11}C-methionine–positive, ^{18}F-FDG–negative extramedullary disease. In the 6 positive controls, ^{18}F-FDG PET/CT revealed the same number of lesions as ^{11}C-methionine PET/CT (all patients had >50 focal lesions on both scans).

Analysis of bone marrow aspirates confirmed monoclonal plasma cells in all 15 cases and demonstrated intense expression of glucose transporter 1 (as the major route of transport of ^{18}F-FDG into the myeloma cell) in all myeloma samples, with little variation between cases (*19*). In analogy to previously published findings of low HK2 expression in false-negative ^{18}F-FDG PET studies (*10*), immunohistochemical analysis of HK2 was performed and also revealed intense enzyme expression by both ^{18}F-FDG PET–negative and ^{18}F-FDG PET–positive samples (median IRS, 9.7 ± 2.4 vs. 10.3 ± 1.9; $P = 0.57$) (Fig. 2; Table 2). To further elucidate the phenomenon of ^{18}F-FDG–negative, viable MM, we focused on G6Pase, an enzyme that hydrolyzes glucose-6-phosphate to free glucose and a phosphate group. Overexpression of G6Pase has been demonstrated as a reason for ^{18}F-FDG negativity in hepatocellular carcinoma, in which low-grade tumors tended to demonstrate higher G6Pase levels than high-grade carcinoma (*21*). However, irrespective of ^{18}F-FDG PET positivity or negativity, G6Pase was highly expressed on myeloma cells in all bone marrow samples, without a significant differences between the 2 cohorts (median IRS, 8.3 ± 2.4 vs. 7.3 ± 2.4; $P = 0.44$) (Fig. 2; Table 2).

DISCUSSION

To our knowledge, this study was the first to investigate protein HK2 and G6Pase expression as an underlying cause for ^{18}F-FDG PET negativity in MM. In contrast to Rasche et al. (*10*), who recently reported on low HK2 gene expression in so-called PET false-negative MM, we did not detect lower HK2 protein levels in ^{18}F-FDG–negative, ^{11}C-methionine–positive patients than in either ^{18}F-FDG– or ^{11}C-methionine–positive controls. Additionally, no significant differences in G6Pase expression between the 2 cohorts could be identified. Thus, additional—yet-unidentified—factors in ^{18}F-FDG negativity must be present. At the moment, although we cannot provide exact explanations for the apparent existence of different ^{18}F-FDG–negative myeloma cell clones, our observation further underscores the distinct heterogeneity of MM (*22–24*). The presence of disease that is viable as detected by whole-body diffusion-weighted MRI (*10,25*) but not positive with ^{18}F-FDG or non–^{18}F-FDG radiotracers, including markers of amino acid and lipid metabolism (e.g., ^{11}C-choline, ^{11}C-acetate) (*11,13*) or of cell membrane receptor expression such as C-X-C motif chemokine receptor 4 (*26,27*), raises the question of distinct biologic subcohorts with distinct behavior and, potentially, distinct susceptibility to therapeutic regimens.

Noteworthy, the present study enrolled mainly patients with relapsed or refractory disease, whereas the previous study (*10*) included subjects with newly diagnosed MM. Thus, it is conceivable that both studies investigated patients with biologically different disease, contributing to the differences observed in both studies. Further research on the biologic and prognostic differences in different morphologic and metabolic disease patterns is required to elucidate the significance of ^{18}F-FDG–negative disease and to aid in further understanding the complexity of myeloma biology. Given the pronounced inter- and intraindividual tumor heterogeneity, it can be assumed that a combination of different imaging approaches might be needed to comprehensively depict MM in a specific patient.

This study has some limitations. First, only a small number of patients could be enrolled, thus limiting statistical power. Second, expression of only 2 proteins was assessed, and no definite explanations

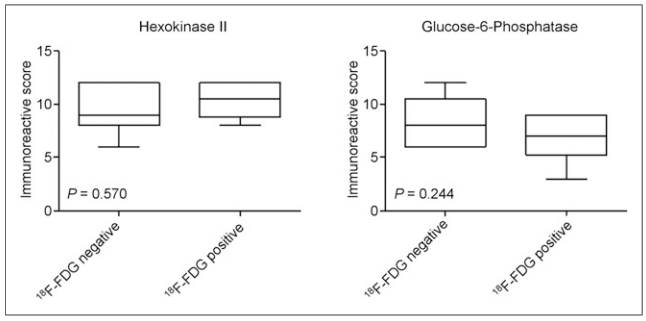

FIGURE 2. Box plot analysis of HK2 and G6Pase levels in ^{18}F-FDG–negative vs. ^{18}F-FDG–positive viable MM (unpaired Student *t* test, 2-tailed).

TABLE 2
Individual Immunohistochemical Results for HK2 and G6Pase

Patient no.	Age (y)	Sex	HK2			G6Pase		
			Positive cells (%)	Intensity	IRS	Positive cells (%)	Intensity	IRS
^{18}F-FDG–negative								
1	67	M	90	3	12	80	2	6
2	56	M	75	3	9	90	3	12
3	63	M	90	3	12	90	3	12
4	62	M	100	3	12	80	3	9
5	53	F	80	2	6	70	2	6
6	63	F	90	2	8	80	2	6
7	53	F	100	3	12	100	2	8
8	64	M	75	2	8	90	2	8
9	62	F	90	2	8	90	2	8
^{18}F-FDG–positive								
C1	64	M	80	3	9	80	2	6
C2	63	M	10	2	8	70	3	9
C3	51	M	100	3	12	70	3	9
C4	73	M	100	3	12	90	2	8
C5	63	F	75	3	9	70	1	3
C6	53	M	100	3	12	80	3	9

for the presence of viable, ^{18}F-FDG–negative MM can be provided. Potentially, bone marrow involvement tended to be lower in ^{18}F-FDG–negative patients than in ^{18}F-FDG–positive patients. However, random bone marrow biopsy is prone to sampling bias, rendering falsely low percentages for malignant plasma cell infiltration. Of note, a patchy pattern of intramedullary involvement was observed in most patients (as assessed by ^{11}C-methionine PET/CT). In addition, serum parameters documented viable myeloma in all subjects. Third, no comparison of PET imaging results to diffusion-weighted MRI was performed. Last, further differences (beyond the inclusion of different patient cohorts) between our study and the study by Rasche et al. (*10*) are to be appreciated: whereas immunohistochemistry on trephine biopsies to investigate differences in HK2 and G6Pase expression was investigated by our group, Rasche et al. used gene expression profiling of CD138 purified plasma cells in a considerably larger patient cohort ($n = 227$).

CONCLUSION

This pilot study reports on the presence of ^{18}F-FDG PET–negative viable myeloma with relatively high expression of HK2 (and G6Pase). Further research to elucidate the underlying mechanisms and prognostic implications of HK2-positive, ^{18}F-FDG–negative MM is highly warranted.

DISCLOSURE

No potential conflict of interest relevant to this article was reported.

REFERENCES

1. Cavo M, Terpos E, Nanni C, et al. Role of ^{18}F-FDG PET/CT in the diagnosis and management of multiple myeloma and other plasma cell disorders: a consensus statement by the International Myeloma Working Group. *Lancet Oncol.* 2017;18:e206–e217.
2. Zamagni E, Patriarca F, Nanni C, et al. Prognostic relevance of 18-F FDG PET/CT in newly diagnosed multiple myeloma patients treated with up-front autologous transplantation. *Blood.* 2011;118:5989–5995.
3. Zamagni E, Nanni C, Gay F, et al. ^{18}F-FDG PET/CT focal, but not osteolytic, lesions predict the progression of smoldering myeloma to active disease. *Leukemia.* 2016;30:417–422.
4. Bartel TB, Haessler J, Brown TL, et al. F18-fluorodeoxyglucose positron emission tomography in the context of other imaging techniques and prognostic factors in multiple myeloma. *Blood.* 2009;114:2068–2076.
5. Moreau P, Attal M, Caillot D, et al. Prospective evaluation of magnetic resonance imaging and [^{18}F]fluorodeoxyglucose positron emission tomography-computed tomography at diagnosis and before maintenance therapy in symptomatic patients with multiple myeloma included in the IFM/DFCI 2009 trial: results of the IMAJEM study. *J Clin Oncol.* 2017;35:2911–2918.
6. Lapa C, Luckerath K, Malzahn U, et al. 18 FDG-PET/CT for prognostic stratification of patients with multiple myeloma relapse after stem cell transplantation. *Oncotarget.* 2014;5:7381–7391.
7. Stolzenburg A, Luckerath K, Samnick S, et al. Prognostic value of [^{18}F]FDG-PET/CT in multiple myeloma patients before and after allogeneic hematopoietic cell transplantation. *Eur J Nucl Med Mol Imaging.* 2018;45:1694–1704.
8. van Lammeren-Venema D, Regelink JC, Riphagen II, Zweegman S, Hoekstra OS, Zijlstra JM. ^{18}F-fluoro-deoxyglucose positron emission tomography in assessment of myeloma-related bone disease: a systematic review. *Cancer.* 2012;118:1971–1981.
9. Zamagni E, Nanni C, Patriarca F, et al. A prospective comparison of ^{18}F-fluorodeoxyglucose positron emission tomography-computed tomography, magnetic resonance imaging and whole-body planar radiographs in the assessment of bone disease in newly diagnosed multiple myeloma. *Haematologica.* 2007;92:50–55.
10. Rasche L, Angtuaco E, McDonald JE, et al. Low expression of hexokinase-2 is associated with false-negative FDG-positron emission tomography in multiple myeloma. *Blood.* 2017;130:30–34.
11. Nanni C, Zamagni E, Cavo M, et al. ^{11}C-choline vs. ^{18}F-FDG PET/CT in assessing bone involvement in patients with multiple myeloma. *World J Surg Oncol.* 2007;5:68.
12. Cassou-Mounat T, Balogova S, Nataf V, et al. ^{18}F-fluorocholine versus ^{18}F-fluorodeoxyglucose for PET/CT imaging in patients with suspected relapsing or progressive multiple myeloma: a pilot study. *Eur J Nucl Med Mol Imaging.* 2016;43:1995–2004.

13. Ho CL, Chen S, Leung YL, et al. ^{11}C-acetate PET/CT for metabolic characterization of multiple myeloma: a comparative study with ^{18}F-FDG PET/CT. *J Nucl Med.* 2014;55:749–752.
14. Dankerl A, Liebisch P, Glatting G, et al. Multiple myeloma: molecular imaging with ^{11}C-methionine PET/CT—initial experience. *Radiology.* 2007;242:498–508.
15. Nakamoto Y, Kurihara K, Nishizawa M, et al. Clinical value of ^{11}C-methionine PET/CT in patients with plasma cell malignancy: comparison with ^{18}F-FDG PET/CT. *Eur J Nucl Med Mol Imaging.* 2013;40:708–715.
16. Lapa C, Knop S, Schreder M, et al. ^{11}C-methionine-PET in multiple myeloma: correlation with clinical parameters and bone marrow involvement. *Theranostics.* 2016;6:254–261.
17. Lapa C, Garcia-Velloso MJ, Luckerath K, et al. C-11-methionine-PET in multiple myeloma: a combined study from two different institutions. *Theranostics.* 2017;7:2956–2964.
18. Lückerath K, Lapa C, Albert C, et al. C-11-methionine-PET: a novel and sensitive tool for monitoring of early response to treatment in multiple myeloma. *Oncotarget.* 2015;6:8418–8429.
19. Lapa C, Schreder M, Luckerath K, et al. [^{11}C]methionine emerges as a new biomarker for tracking active myeloma lesions. *Br J Haematol.* 2018;181:701–703.
20. Remmele W, Stegner HE. Recommendation for uniform definition of an immunoreactive score (IRS) for immunohistochemical estrogen receptor detection (ER-ICA) in breast cancer tissue [in German]. *Pathologe.* 1987;8:138–140.
21. Torizuka T, Tamaki N, Inokuma T, et al. In vivo assessment of glucose metabolism in hepatocellular carcinoma with FDG-PET. *J Nucl Med.* 1995;36:1811–1817.
22. Lapa C, Schirbel A, Samnick S, et al. The gross picture: intraindividual tumour heterogeneity in a patient with nonsecretory multiple myeloma. *Eur J Nucl Med Mol Imaging.* 2017;44:1097–1098.
23. Rasche L, Chavan SS, Stephens OW, et al. Spatial genomic heterogeneity in multiple myeloma revealed by multi-region sequencing. *Nat Commun.* 2017;8:268.
24. Bolli N, Avet-Loiseau H, Wedge DC, et al. Heterogeneity of genomic evolution and mutational profiles in multiple myeloma. *Nat Commun.* 2014;5:2997.
25. Dimopoulos MA, Hillengass J, Usmani S, et al. Role of magnetic resonance imaging in the management of patients with multiple myeloma: a consensus statement. *J Clin Oncol.* 2015;33:657–664.
26. Lapa C, Schreder M, Schirbel A, et al. [^{68}Ga]pentixafor-PET/CT for imaging of chemokine receptor CXCR4 expression in multiple myeloma: comparison to [^{18}F]FDG and laboratory values. *Theranostics.* 2017;7:205–212.
27. Philipp-Abbrederis K, Herrmann K, Knop S, et al. In vivo molecular imaging of chemokine receptor CXCR4 expression in patients with advanced multiple myeloma. *EMBO Mol Med.* 2015;7:477–487.